

Semi-quantitative temperature accelerated life test (ALT) for the reliability qualification of concentrator solar cells and cell on carriers

Neftali Nuñez, Manuel Vazquez, Vincenzo Orlando *, Pilar Espinet-González and Carlos Algora

Instituto de Energía Solar, Universidad Politécnica de Madrid, Madrid, 28040, Spain

ABSTRACT

An adequate qualification of concentrator photovoltaic solar cells and cell-on-carriers is essential to increase their industrial development. The lack of qualification tests for measuring their reliability together with the fact that conventional accelerated life tests are laborious and time consuming are open issues. Accordingly, in this paper, we propose a semi-quantitative temperature-accelerated life test to qualify solar cells and cell-on-carriers that can assure a minimum life when failure mechanisms are accelerated by temperature under emulated nominal working conditions with an activation energy >0.9 eV. A properly designed semi-quantitative accelerated life test should be able to determine if the device under test will satisfy its reliability requirements with an acceptable uncertainty level. The applicability, procedure, and design of the proposed test are detailed in the paper. Copyright © 2015 John Wiley & Sons, Ltd.

KEYWORDS

reliability; qualification; multijunction solar cells; accelerated life test

*Correspondence

Vincenzo Orlando, Instituto de Energía Solar, Universidad Politécnica de Madrid, Madrid, 28040 Spain.

E-mail: vincenzo.orlando@ies-def.upm.es

1. INTRODUCTION

In recent years, multijunction solar cells (MJSC)-based concentration photovoltaic systems (CPV) have been taking off with the installation of over 50 MW in 2011, over 100 MW in 2012 [1], and 160 MW in 2013 [2]. This rapid evolution is due to an increase in performance (nowadays, there are several multijunction solar cell architectures with efficiencies in the 40–45% range [3]) and a decrease in production and deployment costs. Also, the estimations for energy payback time of CPV commercial systems are 0.9 years. This is half of the payback time of conventional silicon PV system [4].

The current leveled cost of energy for CPV systems is roughly \$0.14/kWh and could be further reduced to \$0.06/kWh [1]. In these economic studies, a warranty time of 30 years is assumed. Therefore, reliability is a key issue in order to improve the competitiveness of CPV systems. However, the reliability of CPV systems has not been extensively studied yet; in fact, CPV is still an emerging technology that has not been in the field long enough. Because of this need, the qualification standard IEC-62108 was created for qualifying CPV systems and assemblies [5].

However, the IEC-62108 does not cover the qualification of the cell-on-carriers (CoC) or solar cells, and there are still many unknowns regarding these components. In fact, there are MJSCs with different architectures, number of subcells, semiconductor materials, encapsulations techniques, concentration levels, sizes, metallic contacts, and so on. Consequently, different MJSC designs could have a very different reliability and failure mechanisms that are still not reported in the literature. So a new standard, namely, IEC-62787 is being developed for the qualification of concentrator solar cells and CoC assemblies. This implies the need to develop new procedures to determine the reliability of the different concentrator MJSCs in a short period of time; thus, this has been an important topic discussed by the CPV community in the last years [6] and has culminated in the development of the upcoming IEC-62787 standard: “Concentrator photovoltaic (CPV) solar cells and cell-on-carrier (CoC) assemblies – Reliability qualification”.

The objective of this work is to propose guidelines to develop a temperature-accelerated life test emulating operating conditions that can guarantee, with an acceptable uncertainty level, a given warranty period under thermal stress. The procedure is simple and short in order to have

an estimation of the reliability for any kind of concentrator solar cell/CoC architecture. That is, the semi-quantitative test that we propose is a pass/fail test, as the other tests to be included in any qualification standard, but in addition, it also determines if the solar cells/CoCs tested will pass their long-term nominal reliability target (which is normally set as X years). The proposed test is intended to help with the determination of the temperature qualification tests that are going to be included in the upcoming IEC-62787 standard.

2. SELECTION OF A SUITABLE STRESS AND TYPE OF ACCELERATED LIFE TESTS

In order to determine the best approach, it is compulsory to discuss the suitability of the different kind of accelerated tests. The first part is to choose between accelerated life test (ALT) and highly accelerated life test (HALT):

- ALT consists on putting a set of devices working in nominal working conditions except for one stressor, which is set to a value higher than nominal. This stress accelerates the life of the devices following several models and/or laws [7]. Depending on the selected stressor, it is possible to accelerate some failure mechanisms or others.
- HALT consists on putting a little number of devices under one or various high stresses and should not be construed as a life test. HALT is a stress test used to determine the operating margins, destructive limits, and a factor of safety of a device. So, HALT is a fast reliability technique used in order to find the predominant failure mechanisms in a product.

It is of high interest to design an accelerated test that allows the qualification of the devices taking into account as reference the total warranty life of the device [8,9]. The best technique to do this is a slower and quantitative ALT test [7,10]. Therefore, we suggest an ALT and not a HALT for the purpose of IEC-62787.

In CPV solar cells and CoCs, thermally activated failures that have appeared either in the field or in the temperature ALTs are (a) shunt perimeter degradation [11–14], which is observed under temperature stress in the ALT and by a combination of temperature, light bias, and moisture in the field [11], and (b) thermal runaway [8,15–17]. From the temperature ALTs, the activation energies obtained for perimeter and thermal runaway failures were 1.02 and 1.58 eV, respectively [8,14]. In the field, thermal runaway failures caused by thermal fatigue are strongly dependent on the presence of moisture and the thermal cycling of the module.

In this paper, a temperature ALT is proposed, with a single test temperature that assures a minimum life for the tested solar cells/CoCs if they pass the qualification test. To do that, an activation energy range wider than the

previously determined activation energies is used, with the goal of taking into account as much types of failure mechanisms that could possibly be detected in the future. This is the base for what we call a semi-quantitative ALT, with a reduced test time and simpler methodology and setup than the common temperature ALT. We mean semi-quantitative in the sense that no specific values are determined but ranges for acceptance or rejection of the product.

As it has been explained previously, this test will be valid for failure mechanisms that are accelerated by temperature under emulated nominal working conditions and must be complemented with other tests that accelerate failure mechanisms affected by other stressors, such as those proposed in the IEC-62787 draft (thermal cycling, damp heat, humidity freeze, etc.).

3. SEMI-QUANTITATIVE TEMPERATURE ACCELERATED LIFE TEST

In order to fulfill the requirements detailed in Section 2, we propose a semi-quantitative test with the following characteristics:

- The solar cells/CoCs will be tested at only one stress temperature.
- The photo-generated current under nominal working conditions (concentration level) will be emulated by means of injected current in darkness. The choice of an adequate electrical stress level is mandatory in order to prevent the appearance of unreal failures. Therefore, injection current has to be carefully chosen as we will see in Section 4.2.
- The test time duration will be fixed in advance, and it will be limited to a few weeks.
- The solar cells will be characterized only before and after the test to determine the number of failures during the tested time.

3.1. Suitability of using forward biasing on the solar cell to emulate photogeneration

Because of the inherent difficulty to illuminate solar cells at very high irradiances (hundred or thousand suns) for hundred or thousand hours while they are stressed at very high temperatures, we think the best way to emulate the electric performance of the cell under concentrated light is by forward biasing, that is, by injecting a current in darkness producing similar effects than those produced by the photo-generated current under concentration as it is described in Section 4.2. Of course, both regimes are not equal, so in this section, we show their equivalences and differences.

Figure 1 shows a one-diode lumped model for a single junction solar cell operating under illumination and at

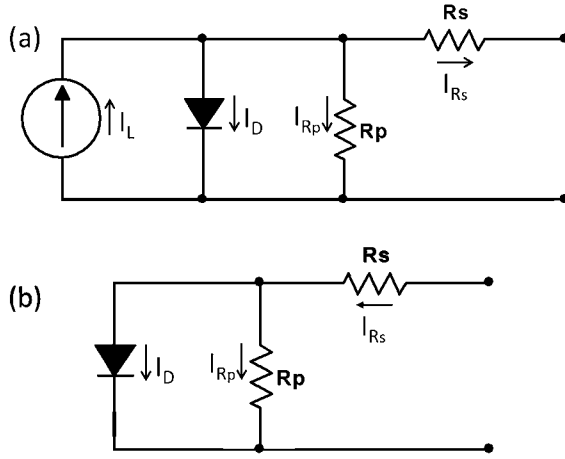


Figure 1. One diode model of a solar cell under illumination (a) and at forward bias (b). In this model, R_s and R_p are lumped parameters collecting all the resistive parts of the solar cell. For each situation, the values of the currents are different.

forward bias. For the sake of simplicity, we will use this model to explain the different operation conditions.

Under normal operation, the solar cells of a concentration system will be paired with a maximum power point tracker, so they will be operating in this bias point for most of their lifetime. In this situation, as shown in Figure 1(a), the current delivered to the external load (I_{RS}) is slightly lower than the photogenerated current (I_L), so, the current flowing through the p-n junction $I_D = I_L - I_{RS}$, which is forward biased, is low. We firstly neglect the current flowing through the parallel resistance (R_p), because otherwise that would mean a faulty solar cell. In any case the unsuitable situation of a non-negligible R_p is also considered in the discussions that follow in this section.

When the solar cell is at forward bias (Figure 1(b)), the diode (i.e., the p-n junction) is also forward biased, but most of the current injected into the solar cell flows through the junction diode ($I_{Rp} \approx 0$, $I_D \approx I_{RS}$). Therefore, both at illumination and at forward biasing the p-n junction is forward biased although it drains different current levels.

At first approach, when the solar cell is at open circuit conditions, most of the photocurrent flows through the diode, and only a small fraction will flow through the parallel resistance and nothing through the series resistance. We have verified this assumption, by using our extended 3D distributed model [18], and we have calculated the voltage loss in the horizontal series resistances of top cell emitter and front metal grid for a $3 \times 3 \text{ mm}^2$ triple junction solar cell working at 1000 suns, resulting in a voltage drop of only 20 mV, that is, 0.6% of the V_{oc} . Therefore, the first approach derived from Figure 1(a) is justified. Conversely, on a solar cell under forward bias, the stress is mostly the same for the series resistance and the junction [19]. So, in a solar cell at open circuit, the p-n junction drains almost the same current than with forward biasing. At short circuit, almost all of the photocurrent circulates through the series resistance, and only a small fraction flows

through the diode and parallel resistance. Therefore, in a solar cell under illumination, depending on its operating conditions, the stress will go majoritarily either on the series resistance (i.e., electrical contacts, top cell emitter, etc.) or on the junction. Accordingly, the current injected to a solar cell when emulating illumination conditions has to be carefully calculated in order to avoid an overstress of any part of the cell, as it is explained in Section 4.2. This always results in an injected current lower than the photogenerated current.

This simple model can be extended to a dual-junction solar cell by adding the tunnel diode (Figure 2). Under illumination, the tunnel diode is forward biased, and it is intended to work at the linear part of its I-V curve (Figure 2(a)). On the other hand, if the solar cell is forward biased, the tunnel diode is reverse biased (Figure 2(b)). The I-V curve of a tunnel diode at reverse biasing is linear and has a very similar slope to that of the linear region in forward bias [20–22], as it is shown in the insets of Figure 2. The bias point under forward and reverse bias will be very similar (if properly calculated using the 3D distributed model) but with opposed signs, meaning that in both cases, it will dissipate a similar power. Because the maximum reverse current (not shown in the inset) is much higher (in absolute value) than the peak current (which limits the linear region in forward bias) [20,23], we do not expect any risk of damaging the tunnel diode when the multi-junction solar cell is forward biased, because the tunnel junction current (in absolute value) in darkness will always be below the peak current. Because the selected criterion is conservative, avoiding electrical overstress, it is possible that the tunnel junction could be under-stressed. We believe that because in both photogeneration and forward biasing conditions the device is working on the linear region, there should not be significant differences in the degradation of the tunnel junctions.

The extension of the model from dual to triple junction solar cells does not add any additional difference between the illumination and biasing regimes.

The situation in which R_p is not high enough (so it can drain a non-negligible current) mainly arises from the appearance of defects in the semiconductor structure of the solar cell. The stress suffered by these defects will be similar both under illumination and at forward bias conditions, except in the case that defects are beneath the bus bar. In this case, the defects would be overstressed at forward bias (because current flows through them) while they would not have a very high stress under illumination conditions (because almost no photogenerated current would pass through them). However, this difference between both regimes is not worrying because in the end, these defects beneath the bus bar could be the seed of failures excited by thermal-mechanical stress and so on under operation conditions. Besides, the failures resulting from these defects are commonly regarded as infant failures [8,15] when forward biasing, and they appear in a very small proportion in commercial cells. This is why the ALT must be carried out on a significant sample size.

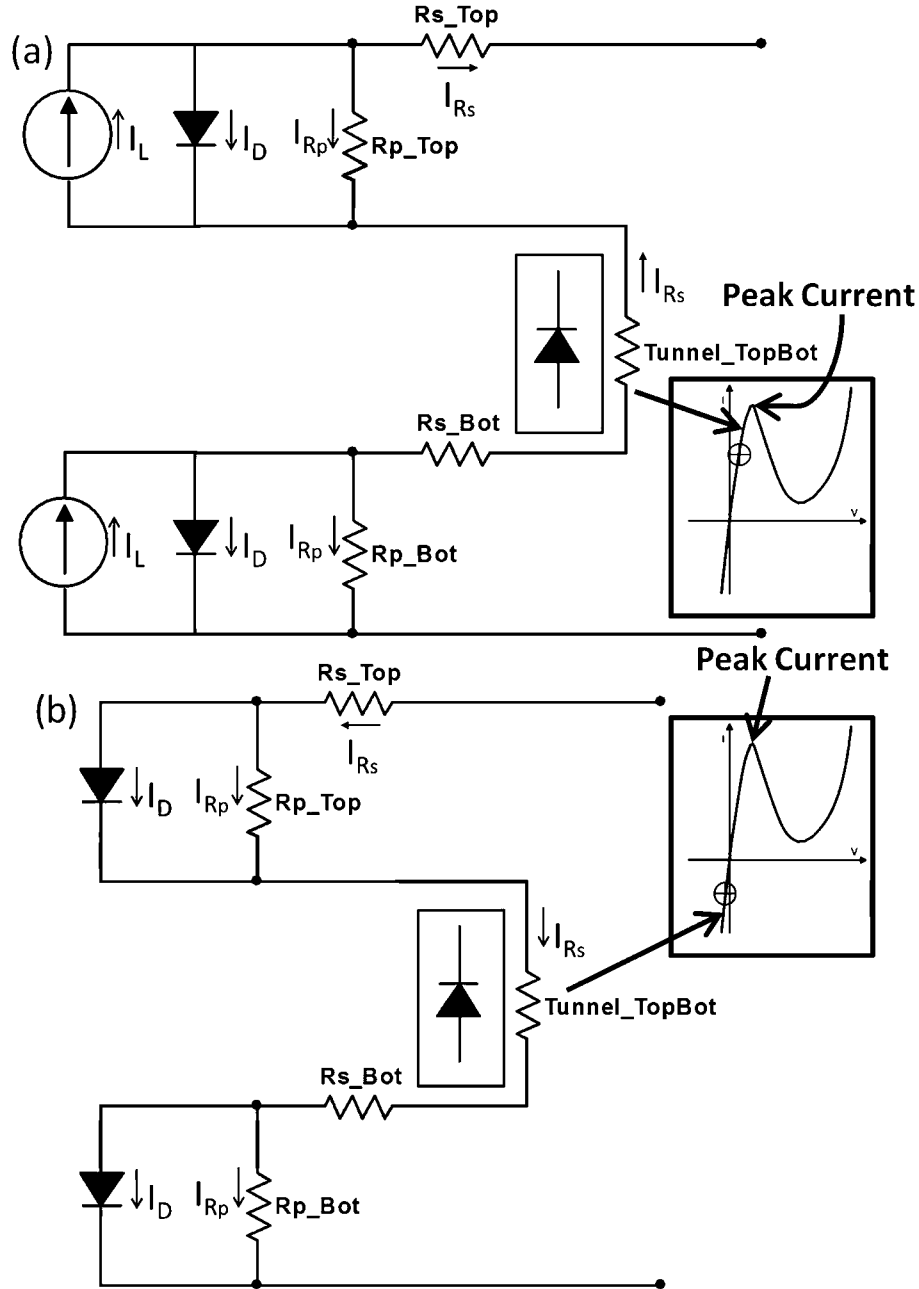


Figure 2. Lumped model of a dual-junction solar cell including tunnel diode under illumination (a) and at forward bias (b). Targets on the I-V curve of the tunnel junction indicate an example of bias points under forward and reverse bias.

Finally, there could be differences between the illumination and forward bias regimes in case of electromigration of the metal contacts because of the inverse current flow of both regimes. Previous works show that electromigration does not happen with the metals used in present commercial III-V concentrator multijunction solar cells (with metallizations based on silver thickening with gold flash) and similar optoelectronic devices [16,24]. Even so, alternative tests would be desirable to dismiss failures because of electromigration using, for example, forward/reverse bias on metallizations.

Accordingly, the use of forward bias seems to be a useful approach for emulating photogeneration conditions in reliability tests, so it is used in the proposed test.

3.2. Assumptions

In order to design a semi-quantitative temperature ALT, the following assumptions have to be taken into account:

- *Life model*: We assume that temperature accelerates the life of the solar cell/CoC following the Arrhenius model [25], as shown in previous temperature ALTs on solar cells/CoCs [8,9,14].

$$L(T) = C \cdot e^{\frac{E_A}{kT}} \quad (1)$$

where $L(T)$ is a temporal measurable characteristic of the life of the device under test which depends on the temperature, k is the Boltzmann constant, E_A is the activation energy of the mechanism which causes the failure and C is a parameter of the Arrhenius model which depends on the $L(T)$ used.

- *Working time*: Concentrator solar cells work only for daylight, and their electricity production is variable, having a peak at about the solar noon. Because of this, we will set that the cells are at nominal working conditions for an average of 5 h each day, which translates to 1825 h per year [8], equivalent to 21% of calendar time. We will refer to this period as “Real Working Time”. This value could be finely tuned to different locations, but a 5 h per day is a good average for places suited for CPV deployment.
- *Reliability distribution function ($R(t)$)*: In this work, it will be assumed that the solar cells/CoC reliability follows a Weibull distribution function with two parameters as also shown in previous works [8,14]. The Weibull distribution is a versatile distribution function that fits very well the reliability of different devices.

$$R(t) = 1 - F(t) = \exp \left[- \left(\frac{t}{\eta} \right)^\beta \right] \quad (2)$$

where $F(t)$ is the accumulated failure probability function, also called unreliability, t is the time, β is the shape parameter, and η is the scale parameter.

3.3. Procedure

In order to carry out the semi-quantitative ALT, several parameters have to be fixed. In this section, the parameters will be fixed with reasonable values with data obtained from previous reliability tests in concentrator solar cells/CoCs [8,14]. In Section 4, the influence of these values on the design of the test will be pointed out.

The semi-quantitative ALT proposal assumes that there is no exact knowledge for both E_A and β for the solar cells under test. Consequently, the following actions about β and E_A are taken:

- *Weibull shape parameter (β)*: Concentrator solar cells/CoCs are devices working at high temperature and current stress. Because of these working conditions, they typically have an increasing failure rate (namely, wear-out mode, $\beta > 1$) [8,9,14], so in this analysis, we have studied two extreme values for this situation, $\beta = 1$ and $\beta = 5$. For $\beta = 1$, the devices have

constant failure rate which corresponds with devices of low electric and thermal stress. For $\beta > 1$, the devices have an increasing failure rate which corresponds with high stress and degradation during the lifetime of the devices. For $\beta < 1$, the devices have a decreasing failure rate, and these failures are considered as infant failures. These failures are usually due to manufacturing weaknesses that must be addressed with a quality screening process, which is carried out before the qualification stage. If many solar cells have a relevant percentage of infant failures, they would not pass the proposed test, because the added failures will appear during the first hours of test.

- *Activation energy*: In this analysis, we have selected a wide range of activation energy values based on our experience on concentrator solar cells/CoCs and similar optoelectronic devices [8,13,14,24,26]. The activation energy range studied is from 0.9 to 1.6 eV. This range should cover almost every failure mechanism affected by temperature.

Another important parameter to design the test is the *stress temperature*, which is the temperature that will accelerate the degradation of the devices under test. The relation between the time at nominal working temperature and the time at a stress temperature is obtained based on the Arrhenius model from the acceleration factor (A_F) due because of changes in the working temperature [27].

$$\begin{aligned} A_F &= L(T_{\text{nom}})/L(T_{\text{stress}}) = \exp \left[\frac{E_a}{k} \left(\frac{1}{T_{\text{nom}}} - \frac{1}{T_{\text{stress}}} \right) \right] \\ &= \exp \left[\frac{E_a}{kT_{\text{nom}}} \left(1 - \frac{T_{\text{nom}}}{T_{\text{nom}} + \Delta T} \right) \right] \end{aligned} \quad (3)$$

where E_a is the activation energy, k is the Boltzmann's constant, T_{nom} is the nominal working temperature of the device, T_{stress} is the temperature at which the device is tested, and ΔT is the temperature increment over T_{nom} .

A *reliability target* must be fixed. As an example, we chose the reliability target as 10% of failures during 25 years of working time, that is $F(t=25 \text{ years})=10\%$.

In order to show the philosophy of the proposed test, two Weibull plots for the unreliability, $F(t)$, have been represented in Figures 3 and 4 in order to simulate two real tests at two different ΔT .

Figure 3 shows the Weibull plot of an accelerated test with a $\Delta T = 35^\circ\text{C}$ higher than T_{nom} , which is assumed to be 80°C [28]. The x-axis represents test time. Once the reliability test is over, the unreliability goal of $F(25 \text{ years}) = 10\%$ is presented as a black point by assuming a 5 h/day operation, resulting in $F(45625 \text{ h}) = 10\%$. From this black point, we use the acceleration factor value (Eq. (3)) by assuming $T_{\text{nom}} = 80^\circ\text{C}$ together with a $\Delta T = 35^\circ\text{C}$. Because we are considering two activation energy limits ranging from 0.9 to 1.6 eV, we will acquire two different points by using $A_F(E_A = 1.6 \text{ eV})$ and $A_F(E_A = 0.9 \text{ eV})$. Each of these two points will generate two straight lines for $\beta = 1$ and 5,

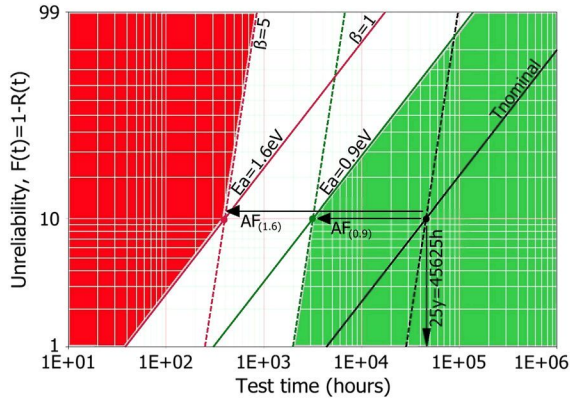


Figure 3. Unreliability versus test time for a $\Delta T = 35^\circ\text{C}$ over $T_{\text{nom}} = 80^\circ\text{C}$.

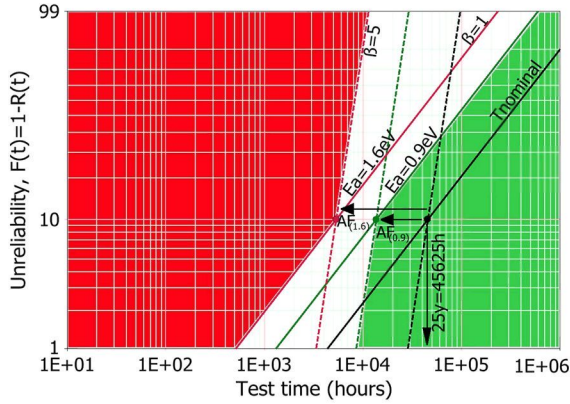


Figure 4. Unreliability versus test time for $\Delta T = 15^\circ\text{C}$ over $T_{\text{nom}} = 80^\circ\text{C}$ for the same assumptions about the E_a , β , and $F(t = 25 \text{ years})$ than in Figure 3.

following Eq. (2). It must be highlighted that calculating the η Weibull parameter is not necessary because our analysis is performed for $F(t = 25 \text{ years}) = 10\%$.

The dotted lines in red and green represent the unreliability target (10% of failures) after working 25 years for the activation energies of 1.6 and 0.9 eV, respectively, that is, corrected by their corresponding A_F . The color coded (red for $E_a = 1.6 \text{ eV}$ and green for $E_a = 0.9 \text{ eV}$) solid lines show the unreliability for different tested hours assuming a shape parameter $\beta = 1$. The color coded dotted lines reproduce the unreliability for a shape parameter $\beta = 5$.

Once the reliability test is over, the unreliability of the solar cell/CoC tested is represented in Figure 3 by a dot. This dot can be placed in three different regions:

- (1) The dot is placed in the green region. This is called the “pass” region because in this case, it is possible to assure that the reliability target (in this case 10% of failures after working 25 years) will be achieved in any case. Therefore, the solar cells/CoCs have passed the qualification test.

- (2) The dot is placed in the red region. In this situation, the reliability target will not be achieved in any case. This is called the “fail” zone because the solar cells/CoCs have not passed the qualification test.
- (3) The dot is placed in the white region. This is called the “uncertainty” region because in this situation, it is not possible to assure if the reliability target is achieved or not for the proposed β and E_a range.

The uncertainty region will change in size depending on the selected ΔT . Accordingly, Figure 4 shows a Weibull plot for $\Delta T = 15^\circ\text{C}$. The decrease in the uncertainty region is clearly shown.

4. DESIGN OF THE SEMI-QUANTITATIVE TEMPERATURE ALT

As pointed out in the previous section. In order to design a qualification test based on ALT, some parameters have to be defined beforehand. In this section, we will further discuss the influence of ΔT and how to determine the injected current.

4.1. Influence of the temperature increment over the nominal working temperature, ΔT

Figures 3 and 4 showed that the uncertainty region changed in size with the selected ΔT over $T_{\text{nom}} = 80^\circ\text{C}$. Therefore, this also affects the test duration. Figure 5 shows how the test time decreases and the uncertainty increases with the temperature increment. To further explain this issue, Figures 6 and 7 show the test time equivalent to 25 years of working time for $\Delta T = 15$ and 35°C , respectively, assuming the corresponding A_F .

The analysis of these figures shows that it is not possible to choose a unique test duration that will fulfill the reliability target for the full range of activation energy values. This is caused by the selected activation energy

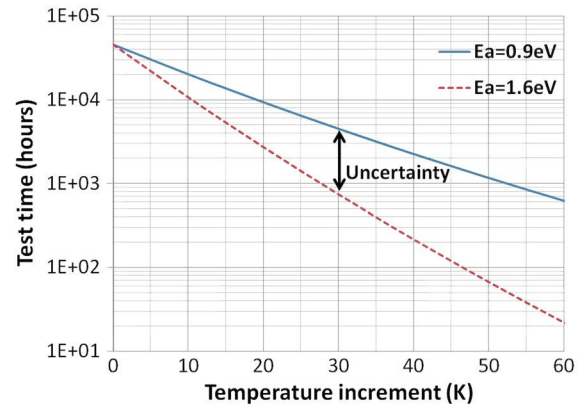


Figure 5. Test time versus ΔT over $T_{\text{nom}} = 80^\circ\text{C}$ for the two extreme E_a values for $F(25 \text{ years}) = 10\%$.

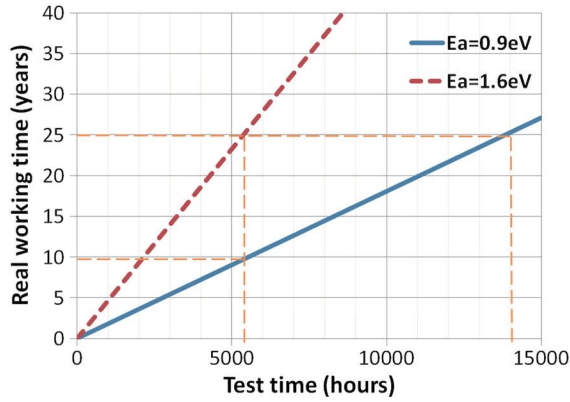


Figure 6. Working time (assuming 5 h/day operation) versus test time for $\Delta T = 15^\circ\text{C}$ over $T_{\text{nom}} = 80^\circ\text{C}$.

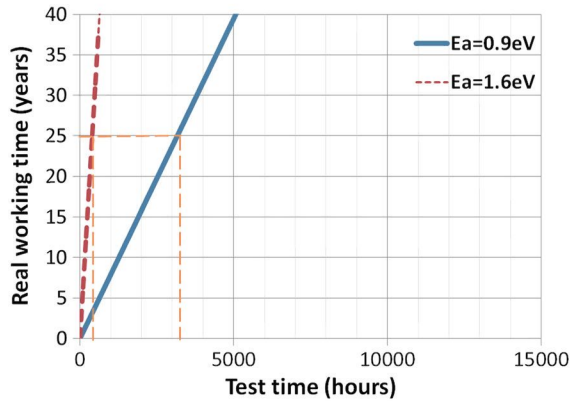


Figure 7. Working time (assuming 5 h/day operation) versus test time for $\Delta T = 35^\circ\text{C}$ over $T_{\text{nom}} = 80^\circ\text{C}$.

range and can be improved if further knowledge about the devices is obtained.

For example, in Figure 6, where $\Delta T = 15^\circ\text{C}$, the choice of a test time at 1.6 eV for 25 years of working time (roughly 5300 h of test time, an excessive test duration) is equal to less than 10 years at 0.9 eV. Figure 7 shows that testing with $\Delta T = 35^\circ\text{C}$ and assuming 1.6 eV for 25 years working time, the test period only considers around 3 years of life at 0.9 eV. This is insufficient for a qualification test requirement.

This means that the final test will need a compromise between manufacturer risk (that a device that fulfills the reliability target is rejected), consumer risk, (that a device that does not fulfill the qualification target is accepted), and cost (simple implementation and a short test duration).

Another important factor is the temperature increment caused by biasing: in order to accelerate the life of the solar cells/CoCs, they will be typically placed inside a climatic chamber. Once inside the climatic chamber, current is injected into the solar cells, heating them up. Depending on the size of the solar cell, the heat sink/CoC size, and the level of current injected, the cell temperature can greatly differ from the set temperature of the climatic

chamber. In order to carry out valid reliability or qualification analysis, the increment in the cell temperature because of power dissipation during current injection must be accurately known

To accurately simulate working conditions, we suggest adding a heat sink for CoC circuits. Another benefit of using heat sinks is a higher thermal inertia, allowing slower temperature gradients during the on/off cycles (injection of current/non-injection of current), isolating temperature-accelerated mechanisms over those of thermal cycling, which are considered in another test in the proposed standard (IEC-62787).

4.2. Determination of the injected current

Controlling the temperature of the solar cells and determining the proper level of current which has to be injected in darkness to avoid overstressing the solar cell are critical set-up parameters of the test. Therefore, in this section, we give some general guidelines to follow in the design of the proposed semi-quantitative ALT.

To emulate the photocurrent of the cells inside the climatic chamber, it is necessary to know beforehand the nominal working conditions under concentration, and with this information, the current to be injected in darkness can be obtained.

In IEC-62108 qualification tests, an injected current of $1.25 I_{\text{SC}}$ (short circuit current) is used for thermal cycling tests. This current value was selected to cause thermal and mechanical stress in the solar cell and assembly, but not to emulate nominal working conditions, which is the objective of the proposed test. Therefore, the $1.25 I_{\text{SC}}$ value cannot be used in the present proposal to emulate the nominal working conditions of the solar cells/CoCs, because depending on the device size, front grid, concentration level, and so on, the current density distribution varies. In order to determine the right forward injection current level, we use our 3D distributed model for triple-junction solar cells to obtain the equivalent current that has to be injected in darkness for several solar cell sizes. This model has been successfully used in previous reliability analysis of triple junction solar cells [8,9].

We have simulated the equivalent injection current required to emulate the operation at two concentrations (500 X and 1000 X) of standard GaInP/Ga(In)As/Ge triple-junction solar cells of different sizes. For the sake of simplicity, all the solar cells simulated have a comb-like front metal grid. The bus bar width is $100\mu\text{m}$ for devices under 30 mm^2 and $250\mu\text{m}$ for devices over 30 mm^2 . The fingers width is fixed to $5\mu\text{m}$ in all the devices. The number of fingers has been optimized for every size and for both concentrations (assuming uniform irradiance).

Once the optimum front grid was determined for each size and concentration, the level of current which has to be injected in darkness has been established by analyzing the current distribution in darkness. The criterion followed is that the level of current which has to be injected in darkness is the highest one which makes that the current density injected does not surpass the current density

photogenerated at any point of the solar cell. This guarantees that no part of the solar cell is overstressed, although some are under-stressed. Therefore, this is a conservative criterion. An alternative option would consist of injecting a current which makes that the minimum current density is the photogenerated current density, but this will cause electrical overstress in some parts of the solar cell [8]. In Figure 8, we present the results obtained from the simulations. The current which has to be injected in solar cells of different sizes follows a sub-linear behavior because of crowding effects. Because of this, the current injected in darkness I_{dark} to the short circuit current at a concentration X $I_{\text{sc}@X}$ ratio is about 0.5 except for the smallest cell sizes.

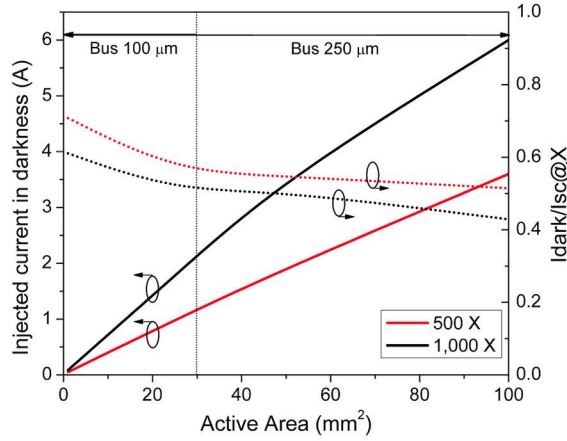


Figure 8. (Left axis) Injected current in darkness, I_{dark} , in triple-junction solar cells of different sizes for emulating two nominal working concentrations: 500 X (red solid line) and 1000 X (black solid line). (Right axis), Corresponding I_{dark} to $I_{\text{sc}@X}$ ratio for emulating two nominal working concentrations: 500 X (red dotted line) and 1000 X (black dotted line).

Finally, it has to be pointed out that different architectures of solar cells could lead to different results but can be calculated by using the method presented here.

5. GUIDELINES

With all the details discussed in the previous sections, it is possible to design the semi-quantitative ALT for the reliability target. We recommend a significant sample size (100 CoCs/solar cells [28]) that is a statistically significant number and that could allow a few possible infant failures.

With the information obtained in Section 4.1 from Figures 5–7, we choose $\Delta T = 25^\circ\text{C}$, because it is a good compromise between the duration of the test (1414 h, equivalent to a 2-month test) and the uncertainty. Figure 9 shows the implications of selecting this temperature increment: the left part of Figure 9 shows a plot of the test time needed to qualify a set of solar cells if their activation energy is 1.6 eV as a function of the selected temperature increment over $T_{\text{nom}} = 80^\circ\text{C}$ if the goal is 90% reliability at 25 years. On the other hand, the right part of Figure 9 shows the equivalent lifetime of solar cells (different of 25 years) for the selected test time in the left figure as a function of the activation energy when it is lower than 1.6 eV. For example, if we select $\Delta T = 25^\circ\text{C}$ on the left curve, the corresponding test time is 1414 h. Now following the horizontal red arrow, we intersect the curve of the activation energy, for example 1.25 eV, and then following the downward red arrow, we find the equivalent lifetime of the solar cell, that is, 11.7 years (instead of 25 years).

Therefore, the two cases (namely, unknown activation energy and known activation energy) that arise for the determination of the main parameters of the test are analyzed in the sections that follow:

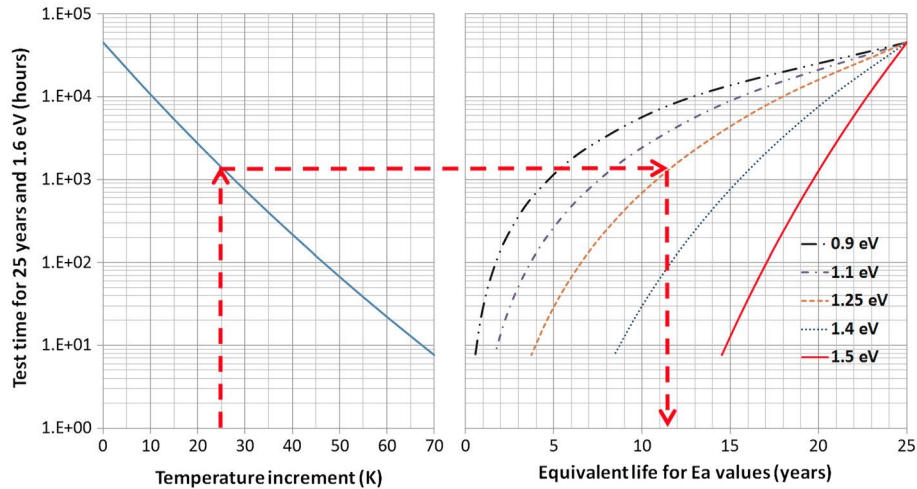


Figure 9. Test time for an activation energy of 1.6 eV, 90% reliability at 25 years and $T_{\text{nom}} = 80^\circ\text{C}$ as a function of the temperature increment of the test (left). Conversion of the equivalent lifetime for different activation energies (right) by following the red arrow (see text for more details).

5.1. Unknown activation energy

If the activation energy of the device is unknown, the device will be qualified between 5.5 (0.9 eV) and 25 years (1.6 eV) with a median value of 11.7 years (1.25 eV) (Figure 9). These lifetimes seem suitable for a qualification test considering the high degree of uncertainties. This is the typical case of many commercial productions at the beginning.

5.2. Known activation energy

This is the desired situation, because the uncertainty is eliminated and the parameters of the test can be accurately determined. The activation energy of the solar cells can be obtained by carrying out ALT tests [7,8,14]). Figure 10 can be used to determine the test parameters, which shows a representation of the Arrhenius model assuming a $T_{nom}=80^{\circ}\text{C}$ for several activation energies, and the equation:

$$t_p = Y_w / A_{FCC} \quad (4)$$

where t_p is the test time in hours, Y_w is the equivalent working time in hours and A_{FCC} is the acceleration factor assuming 5 h of nominal working conditions per day. The first step is to select the known activation energy and a temperature increment over $T_{nom}=80^{\circ}\text{C}$. With these values, the acceleration factor is obtained by using Figure 10. This acceleration factor together with the desired qualification time gives the required test time by using Eq. (4). For example, for 1.25 eV and $\Delta T=60^{\circ}\text{C}$, we obtain $A_{FCC}=390$ in Figure 10 that together with a desired qualification time of 25 years results in a test time of 562 h by using Eq. (4).

Therefore, the determination of the activation energy of a type of solar cell is highly useful and allows a complete

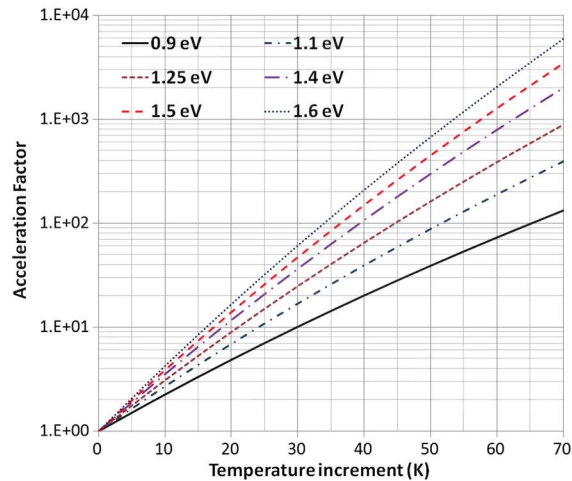


Figure 10. Acceleration factor versus temperature increment over $T_{nom}=80^{\circ}\text{C}$ for several activation energy values.

specification of the qualification test parameters. Anyway, in case of uncertainty of the activation energy value, our proposal also provides the guidelines for the qualification test within an acceptable range.

6. CONCLUSIONS

In this paper, a qualification test procedure for CPV solar cells/CoC based on a temperature ALT with current injection in darkness is proposed. The procedure is short and simple, trying to comply with the needs of the upcoming IEC-62787 standard. The suitability of using forward biasing to emulate photogeneration is shown. Analysis of the key aspects involved in the test with special focus on the injected current and the management of the temperature increment of the solar cells inside the climatic chamber is discussed.

The proposed test estimates the sensitivity of concentrator solar cells and CoCs to physical and chemical degradation processes affected by temperature that occur in emulated nominal working conditions, following the Arrhenius model. Therefore, this test is complementary to other tests that are being considering in the upcoming IEC-62787 standard.

The unknown values of the failure activation energy and Weibull shape parameter for the devices under test causes an uncertainty which is discussed.

A complete test is proposed by assuming specific values of reliability goal (90%), solar cell operation temperature (80°C), and so on, resulting in 1414 h test for 100 tested cells. Also, if the failure activation energy is known, a simple procedure to obtain the test time for a desired qualification time based on the Arrhenius model is presented.

The values proposed are realistic examples in order to explain the presented qualification procedure but other values could be adopted.

ACKNOWLEDGEMENTS

This work has been supported by the European Commission through the funding of the project ENER/FP7/295985/“ECOSOLE”, by the Spanish MINECO through the projects TEC2011-28639-C02-01 and IPT-2011-1408-420000, and by the Comunidad de Madrid through the project MADRID-PV (S2013/MAE-2780).

REFERENCES

1. McConnell R, Garboushian V, Gordon R, Dutra D, Kinsey G, Geer S, Gomez H, Cameron C. *Low-Cost High-Concentration Photovoltaic Systems for Utility Power Generation*. Amonix, Inc., 2012. DOI:10.2172/1040623

2. Cassell J. Concentrated photovoltaic solar installations set to boom in the coming years PV (CPV), IHS Report, 2013.
3. Green MA, Emery K, Hishikawa Y, Warta W, Dunlop ED. Solar cell efficiency tables (version 44). *Progress in Photovoltaics: Research and Applications* 2014; **22**: 701–710.
4. Fthenakis VM, Kim HC. Life cycle assessment of high-concentration photovoltaic systems. *Progress in Photovoltaics: Research and Applications* 2013; **21**: 379–388.
5. IEC 62108 – concentrator photovoltaic (CPV) modules and assemblies – design qualification and type approval, International Electrotechnical Commission, 2007.
6. Kurtz S. International quality assurance standards, NREL, Photovoltaic Module Reliability Workshop, February 16–17, 2011.
7. Nelson WB. *Accelerated Testing: Statistical Models, Test Plans, and Data Analysis*. John Wiley & Sons: Hoboken, NJ, USA, 2009.
8. Espinet-González P, Algora C, Núñez N, Orlando V, Vázquez M, Bautista J, Araki K. Temperature accelerated life test on commercial concentrator III–V triple-junction solar cells and reliability analysis as a function of the operating temperature. *Progress in Photovoltaics: Research and Applications* 2015; **23**: 559–569.
9. Orlando V, Espinet P, Nuñez N, Eltermann F, Contreras Y, Bautista J, *et al.* Preliminary temperature accelerated life test (ALT) on lattice mismatched triple-junction concentrator solar cells-on-carriers, in 10th International Conference on Concentrator Photovoltaic Systems: CPV-10, 2014; 250–253.
10. Suhir E. Accelerated life testing (ALT) in microelectronics and photonics: its role, attributes, challenges, pitfalls, and interaction with qualification tests. *Journal of Electronic Packaging* 2002; **124**: 281–291.
11. Bosco N, Kurtz S. *CPV Cell Characterization Following One-Year Exposure in Golden, Colorado: Preprint*. National Renewable Energy Laboratory (NREL): Golden, CO., 2014.
12. Espinet P, Algora C, González JR, Núñez N, Vázquez M. Degradation mechanism analysis in temperature stress tests on III–V ultra-high concentrator solar cells using a 3D distributed model. *Microelectronics Reliability* 2010; **50**: 1875–1879.
13. González JR, Vázquez M, Núñez N, Algora C, Rey-Stolle I, Galiana B. Reliability analysis of temperature step-stress tests on III–V high concentrator solar cells. *Microelectronics Reliability* 2009; **49**: 673–680.
14. Núñez N, González J, Vázquez M, Algora C, Espinet P. Evaluation of the reliability of high concentrator GaAs solar cells by means of temperature accelerated aging tests. *Progress in Photovoltaics: Research and Applications* 2013; **21**: 1104–1113.
15. Bosco N, Sweet C, Ludowise M, Kurtz S. An infant mortality study of III–V multijunction concentrator cells. *IEEE Journal of Photovoltaics* 2012; **2**: 411–416.
16. Espinet-Gonzalez P, Romero R, Orlando V, Gabas M, Nunez N, Vazquez M, *et al.* Case study in failure analysis of accelerated life tests (ALT) on III-V commercial triple-junction concentrator solar cells, in Photovoltaic Specialists Conference (PVSC), 2013 IEEE 39th, Tampa, FL, 2013; 1666–1671.
17. Muller M. Experience with CPV Module Failures at NREL, NREL, Reliability Workshop, March 1, 2012.
18. Garcia I, Espinet-González P, Rey-Stolle I, Algora C. Analysis of chromatic aberration effects in triple-junction solar cells using advanced distributed models. *IEEE Journal of Photovoltaics* 2011; **1**: 219–224.
19. Vázquez M, Algora C, Rey-Stolle I, González JR. III-V concentrator solar cell reliability prediction based on quantitative LED reliability data. *Progress in Photovoltaics: Research and Applications* 2007; **15**: 477–491.
20. Bertness K, Friedman D, Olson J. Tunnel junction interconnects in GaAs-based multijunction solar cells, in Photovoltaic Energy Conversion, 1994., Conference Record of the Twenty Fourth. IEEE Photovoltaic Specialists Conference-1994, 1994 IEEE First World Conference on, 1994; 1859–1862.
21. Gold RD, Weisberg LR. Permanent degradation of GaAs tunnel diodes. *Solid-State Electronics* 1964; **7**: 811–821.
22. Hayes R, Gibart P, Chevrier J, Wagner S. A stability criterion for tunnel diode interconnect junctions in cascade solar cells. *Solar Cells* 1985; **15**: 231–238.
23. Germanium Power Devices Corp. 1N3712-20 Tunnel Diode. Available: <http://www.digchip.com/datasheets/parts/datasheet/922/1N3713-21.php> (2014, October 14)
24. Fukuda M. *Reliability and degradation of semiconductor lasers and LEDs*. Artech House: Boston, MA, USA, 1991.
25. Arrhenius S. Über die Reaktionsgeschwindigkeit bei der Inversion von Rohrzucker durch Säuren, Zeitschrift für physikalische Chemie, vol. **4**, 1889; pp. 226–248, Translated into English in Selected Readings in Chemical Kinetics, edited by M. H. Back and K. J. Laidler, Oxford: Pergamon, NY, 1967.
26. Kececioglu D. *Reliability and Life Testing Handbook 2*. DEStech Publications, Inc.: Lancaster, PA, USA, 2002.
27. Crowe D, Feinberg A. *Design for Reliability*. CRC Press: Boca Raton, FL, USA, 2010.
28. IEC-62787 Discussion, in IEC Meeting, ed. Albuquerque, New Mexico, 2014.